Civil Engineering Infrastructures Journal, 48(1): 175-188, June 2015
ISSN: 2322-2093

Design of Riprap Stone Around Bridge Piers Using Empirical and Neural Network Method

Karimaee Tabarestani, M.[1*] and Zarrati, A.R.[2*]

[1] Ph.D. of Water Engineering, Civil and Environmental Department, Amirkabir University of Technology, P.O. Box 15915, Tehran, Iran

[2] Professor, Civil and Environmental Department, Amirkabir University of Technology, P.O. Box 15915, Tehran, Iran

Received: 17 Feb. 2014 Revised: 23 Sep. 2014 Accepted: 26 Oct. 2014

Abstract: An attempt was made to develop a method for sizing stable riprap around bridge piers based on a huge amount of experimental data, which is available in the literature. All available experimental data for circular as well as round-nose-and-tail rectangular piers were collected. The data for rectangular piers, with different aspect ratios, aligned with the flow or skewed at different angles to the flow, were used in this analysis. In addition, new experiments were also conducted for larger pier width to riprap size ratio, which was not available in the literature. Based on at least 190 experimental data, the effect of important parameters on riprap stability were studied which showed that the effective pier width is the most effective parameter on riprap stability. In addition, an empirical equation was developed by multiple regression analysis to estimate the stable riprap stone size around bridge piers. The ratio of predicted to experiment riprap size value for all experimental data is larger than one with an average value of 1.75, which is less than many other empirical equations. Finally, in order to achieve a higher accuracy for riprap design, the artificial neural network (ANN) method based on utilizing non-dimensional parameters was deployed. The results showed that the ANN model provides around a 7% improved prediction for riprap size compared to the conventional regression formula.

Keywords: Artificial Neural Network Method, Local Scour, Rectangular and Circular Bridge Pier, Riprap Design, Riprap Stone Stability, Shear Failure

INTRODUCTION

It is estimated that about 60% of bridge failures are due to scouring around their piers and abutments (Shirole and Holt, 1991). Owing to the importance of scouring, a large number of investigations were conducted to understand the mechanism of the scour evolution around bridge piers and abutments in the past decades. Scouring around bridge piers occurs due to a complex flow field with large-scale turbulence structures generated by flow around the pier (Raudkivi, 1998). Notable flow structures are the down flow, horseshoe vortex, water surface roller and wake vortices, as shown in Figure 1. In this figure B: is pier width, L: is pier length Θ: is pier skew angle or flow angle of attack and B_{eff}: is pier effective width.

For a rectangular pier the angle of pier corresponding to the flow plays an important role on the magnitude of effective flow forces. At higher skew angles larger separation areas are expected with stronger wake vortices and a deeper scour hole (Zarrati et al., 2004).

In recent years, a greater attempt was made for prevention of the river bed scouring near bridge piers, and various kinds of revetments have been presented

* Corresponding author Email: m.karimaee@aut.ac.ir

and studied (Parola, 1993; Chiew, 1995; Lauchlan and Melville, 2001; Zarrati et al., 2004; Lagasse et al., 2007; Hosseini, et al., 2011; Karimaee and Zarrati, 2011; Guadio et al., 2012; Tafarojnoruz et al., 2012; Soltani-Gerdefaramarzi et al., 2013; Karimaee and Zarrati, 2013). Among these methods, placing riprap as an armour layer around the pier has been very common.

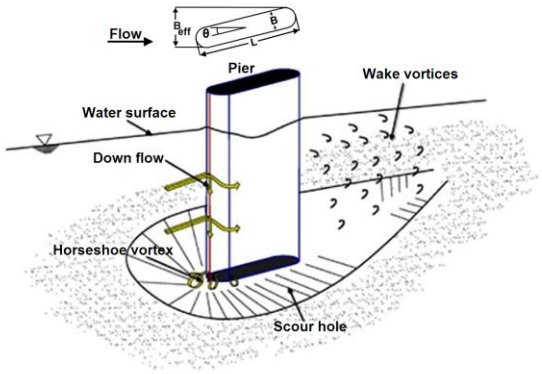

Fig. 1. Schematic layout of flow structure around a rectangular pier.

Many investigations have been carried out to distinguish various parameters that influence the riprap stability and many empirical equations are presented for riprap design against flow forces (Quazi and Peterson, 1974; Parola, 1993; Richardson and Davis, 1995; Lauchlan and Melville, 2001; Lagasse et al., 2007; Mashahir et al., 2009; Karimaee and Zarrati, 2013; Froehlich, 2013). Table 1 summarizes some different equations for the estimation of stable riprap size. Though some empirical equations shown in Table 1 are based on riprap stability number $N_c = \left(U^2 / (SG-1) g \cdot d_{50}\right)$, flow intensity parameter (U/U_c) is also recognized by many investigators as a very effective parameter on the depth of the scour hole and stable riprap size around the bridge pier (Chiew and Melville, 1987; Chiew, 1995; Mashahir et al., 2009), where U: is undisturbed approach mean flow velocity and U_c: is critical mean flow velocity for sediment entrainment, SG: is the riprap stones specific gravity, g: is gravitational acceleration and d_{50}: is the median stable riprap size.

It is known that various equations predict different values for stable riprap in the same flow and pier conditions. This may be due to the complexity of the phenomenon and various parameters involved in riprap destabilization. The main complexities originate from the fact that the critical regions around the pier, where the flow forces are the most effective, are different depending on many factors such as pier shape, flow angle of attack, flow depth and even riprap size. Previous studies showed that riprap instability may occur from upstream of bridge piers due to drag force and from downstream of bridge piers due to the combination of drag and wake vortex forces depending on riprap size, pier aspect ratio and flow angle of attack (Zarrati et al., 2010; Karimaee and Zarrati, 2013). Therefore, developing a general model to estimate a reliable stable riprap size around bridge piers becomes a difficult task. The present work is focused on studying important parameters on riprap stability and with using the large amount of available experimental data presenting a more general formulation including regression analysis and, for the first time, artificial neural network (ANN) for riprap stone sizing. It is also intended to compare two major forms of equations for riprap design in this study, which are equations based on riprap stability number and flow intensity parameter. Moreover, as will be shown later, the trial and error processes in equations that are based on flow intensity sometimes do not converge. The formulation of these equations is also corrected in the present work.

RIPRAP FAILURE MECHANISM AND SIZING

Riprap size should be large enough to resist flow forces including the drag force on riprap stones, as well as the suction effect of wake vortices downstream of the

pier (Karimaee and Zarrati, 2013). In addition, in clear water condition, the riprap layer may fail due to winnowing effects and/or edge scour (Chiew, 1995).

Chiew (1995) cited that the stability of riprap stone is directly related to whether the threshold of sediment entrainment of the riprap stones has been exceeded or not. He showed that riprap stone instability around a circular pier occurs at U/U_c>0.3, not considering stone size and flow depth effects. The parameter U_c can be calculated by a method presented by Hager and Oliveto (2002). This method involves three different equations as follows, based on streambed roughness conditions:

$$U_c = 2.33\left(g' \cdot d_{50}\right)^{1/2} \sigma^{1/3} D_*^{-0.25} \left(\frac{R_h}{d_{50}}\right)^{1/6} \quad D_* \le 10 \tag{1}$$

$$U_c = 1.08\left(g' \cdot d_{50}\right)^{1/2} \sigma^{1/3} D_*^{1/12} \left(\frac{R_h}{d_{50}}\right)^{1/6} \quad 10 < D_* < 150 \tag{2}$$

$$U_c = 1.65\left(g' \cdot d_{50}\right)^{1/2} \sigma^{1/3} \left(\frac{R_h}{d_{50}}\right)^{1/6} \quad D_* \ge 150 \tag{3}$$

where g' and D_*: are reduced gravitational acceleration and dimensionless sediment size, which are calculated by the following equations:

Table 1. Empirical equations for riprap design around bridge piers.

Number	Reference	Equation	Pier type
1	Quazi and Peterson (1973)	$U^2/(SG-1)g \cdot d_{50} = 1.14(d_{50}/y)^{-0.20}$	Round-nose-and-tail rectangular
2	Breusers et al. (1977)	$d_{50} = 2.83U^2/(SG-1)g$	Circular
3	Parola (1993)	$d_{50} = 0.71U^2/(SG-1)g$	Circular
4	Richardson and Davis (1995)	$d_{50} = 0.346(K \cdot U)^2/(SG-1)g$	Round-nose-and-tail and rectangular pier
5	Chiew (1995)	$\frac{U}{U_c} = \frac{0.3}{K(B/d_{50}) \times K(y/B)}$	Circular
6	Croad (1997)	$U^2/(SG-1)g \cdot d_{50} = 2.1 \times A(y/d_{50})^{0.17}$	Circular and Rectangular
7	Lauchlan and Melville (2001)	$\frac{d_{50}}{y} = K_Y \cdot (0.3Fr^{1.2})$	Circular
8	Mashahir *et* al. (2010)	$\frac{U}{U_c} = \frac{0.3}{K(B/d_{50}) \times K(y/B) \times K(Rec)}$	Round-nose-and-tail rectangular
9	Karimaee and Zarrati (2013)	$U^2/(SG-1)g \cdot d_{50} = 3.8 \times (B_{eff}/B)^{-1.5} \times (B/d_{50})^{-0.50} \times (y/d_{50})^{0.25}$	Circular and round-nose-and-tail rectangular
10	Froehlich (2013)	$d_{50}/y = K_r \times K_b \times K_\omega \times K_p \times K_s \times K_\alpha \times Fr^3$	Round and Square nose

Note: *y*: is flow depth, *SG*: is specific gravity of riprap stone; *K*: is coefficient of pier shape: 1.5 for round nose and 1.7 for rectangular nose, U/U_c: is the critical flow intensity for riprap failure where U_c: is critical mean flow velocity for riprap movement, which can be calculated from $U_c = 7.66\sqrt{0.056(SG-1)g \cdot d_{50}}\,(y/d_{50})^{1/6}$ (Chiew, 1995), $K(B/d_{50})$, $K(y/B)$ and $K(Rec)$: are sediment size, flow depth, and rectangular pier adjustment factors respectively (*B*: is circular pier diameter or rectangular pier width); *A*: is acceleration factor: 0.45 for circular and 0.35 for rectangular and shaped edged piers, B_{eff}: is effective pier width. In Lauchlan and Melville (2001), K_Y: is adjustment factors for riprap placement depth, and *Fr*: is upstream Froude number. In Froehlich (2013) the factors K_r, K_b, K_ω, K_p, K_s, K_α: are adjustment factors for slope effect, pier width, cross-flow shear, transverse pier spacing, pier shape, pier alignment with the flow and *Fr*: is the Froude number of the flow approaching a bridge pier.

$$g' = \left(\frac{\rho_s}{\rho} - 1\right) \cdot g \quad (4)$$

$$D_* = \left(\frac{g'}{\nu^2}\right)^{1/3} \cdot d_{50} \quad (5)$$

$\sigma = (d_{84}/d_{16})^{0.5}$: is sediment non-uniformity, v: is water kinematic viscosity, R_h: is hydraulic radius of the channel, ρ: is fluid density and ρ_s: is sediment density.

By introducing riprap stone size and flow depth adjustment factors, respectively, Chiew (1995) presented a relationship for determining stable riprap size (Table 1). Mashahir et al. (2009) extended the Chiew (1995) method by introducing a new adjustment factor for riprap stability around a rectangular pier based on the rectangular pier aspect ratio, L/B where L: is the pier length and B: is the pier width, and θ: is pier skew angle (Figure 1). In order to get riprap size based on Chiew (1995) and Mashahir et al. (2009), a trial and error process is necessary that may not converge in small riprap stone size adjustment factors, due to the logarithmic form of its relationship. Therefore, in the present study a new relationship is derived for riprap design based on parameter U/U_c.

DATA COLLECTION AND EXPERIMENTAL SETUP

Table 2 summarizes all experimental data that are available in the literature and are used in the present analysis. In this table, parameters B/d_{50} and y/B: are relative riprap stone size and relative flow depth respectively, where y: is flow depth, B: is rectangular pier width or circular pier diameter and d_{50}: is median riprap stone size. Furthermore, parameter B_{eff}/B: is relative rectangular effective pier width where B_{eff} is:

$$B_{eff} = L \times Sin\theta + B \times (1 - Sin\theta) \quad (6)$$

Chiew and Melville (1987) observed that the effect of B/d_{50} on local scour depth around bridge pier is negligible when $B/d_{50}>50$. However, the highest B/d_{50} that was tested before was 58.85 (Table 2). To check the effect of B/d_{50} on riprap size, two more sets of experiments were carried out for $B/d_{50}=66.67$. Experimental setup in the present study is similar to Karimaee and Zarrati (2013). Figure 2 shows the schematic view of the experimental flume and definition of various parameters in the experiments. The flume had a working section in the form of a recess below its bed, which was filled with sediment and was located 5 m downstream from the flume entrance. Velocity profile measurements with Acoustic Doppler Velocimeter (ADV) near the working section showed that the flow was fully developed. This was also rechecked by a formula suggested by Kirkgoz and Ardichoglu (1997), which showed that the boundary layer develops before the working section. A rectangular sharp crested weir with a manometer was used for measuring the flow discharge at the flume end. Tail water elevation was controlled by a gate at the downstream end of the flume, and the flow depth was measured by a point gauge with an accuracy of ±0.1 mm. A round-nose-and-tail rectangular pier model made from Perspex was used in the present experiments. The aspect ratio, L/B, of this pier was five, with the width B=50 mm. To avoid winnowing failure, the thickness of the riprap layer was selected as $3d_{50}$ (Chiew, 1995). In addition, a screen with a sieve size of 0.3 mm was used between the bed and riprap materials as a filter. In each experiment, in order to prevent the edge failure of the riprap layer, the riprap material was spread over the whole erodible material surface. In this condition, it was possible to test high discharges without the danger of finer bed material being washed away. This setup was therefore suitable to examine the stability of the riprap stones against the flow forces.

Table 2. Results of the experiments.

Test Series No.	Number of Tests	Pier Aspect Ratio	B_{eff}/B	B/d_{50}	y/B	U/U_c	Reference
1	2	5	1	66.7	1.8 3	0.335 0.353	Present Study
2	38	3	1 – 1.68	7.14 - 35.71	1.3 – 3.9	0.28 – 0.64	Karimaee and Zarrati (2013)
3	65	5	1 – 2.37	7.14 - 58.8	1.2 – 4.9	0.29 – 0.65	
4	41	7	1 – 3.05	7.14 - 35.71	1.2 – 4.5	0.24 – 0.63	
5	4	3	1 – 1.68	6.16-14.1	2.6	0.36-0.51	Mashahir et al. (2010)
6	4	5	1 – 2.37	6.16-14.1	2.6	0.36-0.51	
7	4	7	1 – 3.05	6.16-14.1	2.6	0.36-0.51	
8	24	Circular	1	3.64-18.35	3.0-9.88	0.45-0.68	Zarrati et al. (2010)
9	40	1.4 – 7.1	1	8.46	1.0-3.0	0.43 -0.48	Parola (1993)
10	42	2.5	1	4.44 - 24.8	0.65 – 3.14	0.43 – 0.63	Quazi and Petersen (1973)

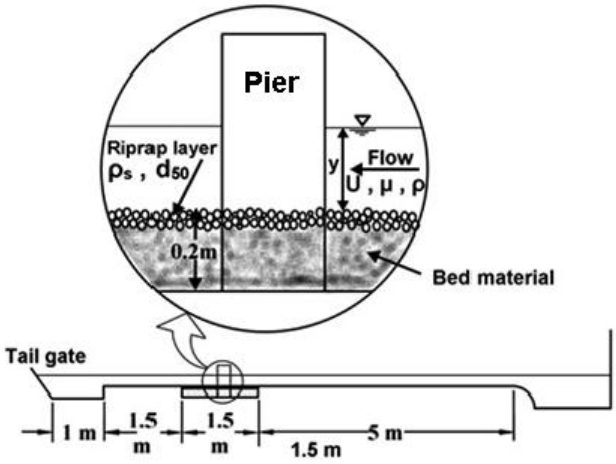

Fig. 2. Laboratory flume and experimental layout (side view).

In each experiment, for a known discharge, the tail water depth was fixed for 15 minutes and, if riprap stones did not move, the depth was decreased gradually by about 5 mm and the experiment continued for another 15 minutes. This procedure continued until the threshold of instability (shear failure) was observed in the riprap layer. Based on previous experiences reported by Chiew (1995), Lauchlan and Melville (2001), and Karimaee and Zarrati (2013), in the present work, the movement of few riprap stones in 15 minutes was considered as the failure criterion. At the failure condition, the flow depth upstream of the pier and the flow discharge were recorded in order to compute the upstream undisturbed flow velocity. Each experiment was repeated at least twice to recheck the results.

More information about the experimental setup and the way of performing the experiments is presented in Karimaee and Zarrati (2013).

RESULTS AND DISCUSSION

Based on dimensional analysis the following relationship can be presented for riprap sizing around a round-nose-and-tail pier based on flow intensity parameters (Chiew, 1995; Mashahir et al., 2009; Karimaee and Zarrati, 2013):

$$\frac{U}{U_c} = f\left(\frac{B}{d_{50}}, \frac{y}{B}, \frac{B_{eff}}{B}\right) \quad (7)$$

where U/U_c: is the flow intensity at the incipient of riprap motion. If U/U_c is calculated then riprap size can be determined from Eqs. (2) to (4). In the following section, by analysing all the collected experimental data in Table 2, the effect of different parameters in Eq. (7) on U/U_c is examined.

Effect of B/d_{50} on U/U_c

Figure 3 shows the effect of parameter B/d_{50} on U/U_c based on the experimental data. The results show that B/d_{50} significantly affects U/U_c for B/d_{50}<50. However, in rectangular piers, such an effect reduces as the skew angle of the pier increases. The significant effect of B/d_{50} in B/d_{50}<50 on local scour around bridge is also reported previously by Chiew and Melville (1987). In contrast, some other researchers such as Lee and Sturm (2009) and Sheppard et al. (2004) observed that the local scour depth around a bridge pier reduces when B/d_{50}>50.

It can be inferred from Figure 3 that by decreasing B/d_{50}, in a constant B_{eff}/B, the parameter U/U_c increases (riprap size decreases). For example, in an aligned rectangular pier, by decreasing the parameter B/d_{50} from 66.7 to 7.14, the value of U/U_c increased by about 82%. However, in higher B_{eff}/B, due to the important effect of this parameter, the effect of B/d_{50} is less evident.

Effect of y/B on U/U_c

Figure 4 shows the effect of parameter y/B on (U/U_c) for a circular pier and for an aligned rectangular pier. It is obvious that the influence of y/B in range of 1.2<y/B<5 on parameter U/U_c is negligible. A similar conclusion was drawn by Zarrati et al. (2010) for the circular pier.

Experimental data show that in skewed rectangular piers y/B has no effect on U/U_c except for B_{eff}/B >3 and B/d_{50}<20 when y/B<3 (higher skew angle and larger riprap size, Figure 5). Based on Karimaee and Zarrati (2013), in this condition the critical region for the riprap stone failure was downstream of the pier due to wake vortices action.

Effect of B_{eff}/B on U/U_c

Figure 6 shows the effect of parameter B_{eff}/B on the instability of the riprap stones. As shown in this figure, for rectangular piers, by increasing B_{eff}/B, U/U_c decreases. This means a constant riprap size is removed in lower flow intensity by increasing the pier skew angle. Experiments show that, in the case of B/d_{50}=35.71, by increasing the parameter B_{eff}/B from 1 to 3.4, the parameter U/U_c decreased by about 45%. It is interesting to note that by increasing B_{eff}/B the critical region for riprap incipient motion moves towards downstream of the pier (Karimaee and Zarrati, 2013).

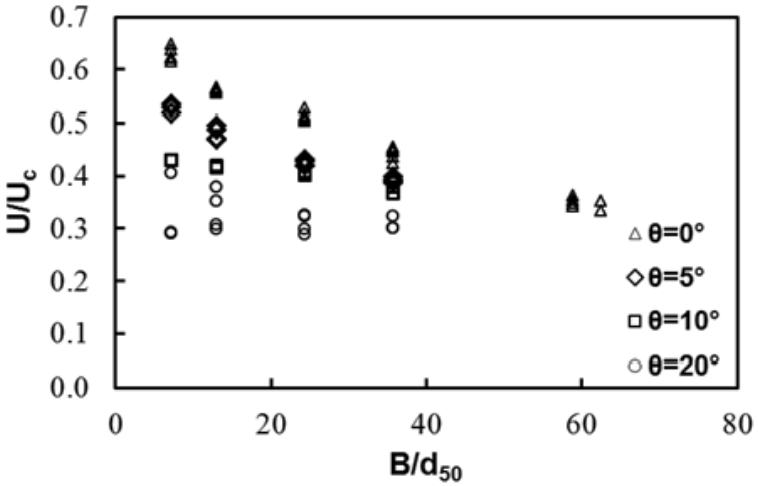

Fig. 3. Effect of parameter B/d_{50} on critical U/U_c at different pier skew angles for pier L/B=5.

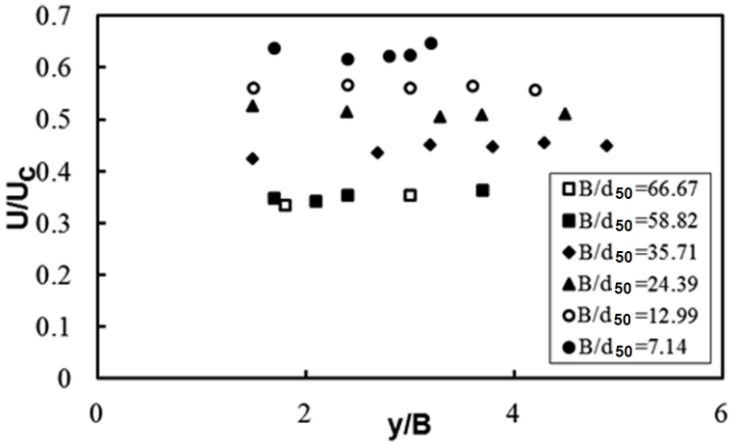

Fig. 4. Effect of parameter y/B on critical U/U_c at aligned rectangular piers.

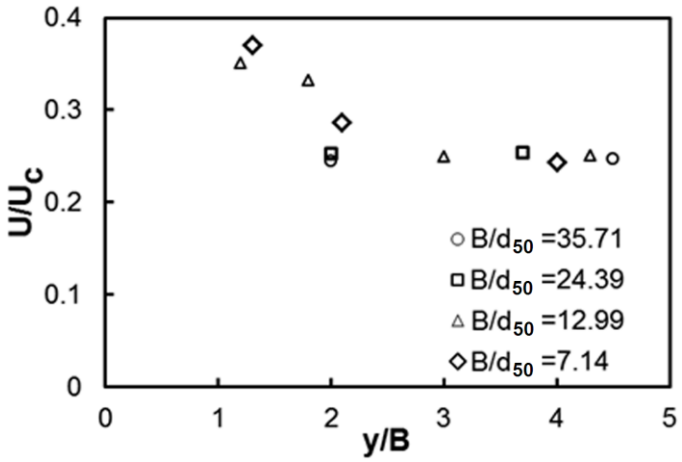

Fig. 5. Effect of parameter y/B on critical U/U_c at B_{eff}/B=3.05.

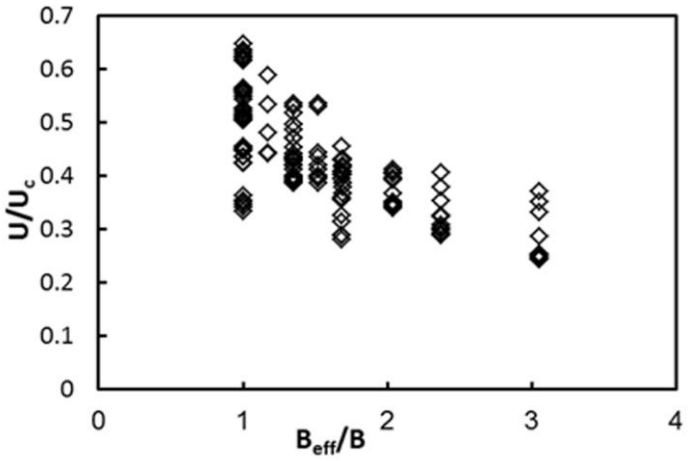

Fig. 6. Effect of parameter B_{eff}/B on critical U/U_c.

RIPRAP DESIGN METHOD

Experimental data analysis in Table 2 shows that while B/d_{50}>50 for B_{eff}/B=1, the parameter U/U_c for the riprap instability condition remained constant at the value of 0.35. However, by decreasing B/d_{50} from 50, the parameter U/U_c increases.

By analysing the experimental data, the following equations can be developed in order to find the critical riprap stone around a pier:

$$\frac{U}{U_c}=\frac{0.35}{K\left(\frac{B_{eff}}{B}\right)\times K\left(\frac{B}{d_{50}}\right)} \quad (8)$$

$$K\left(\frac{B_{eff}}{B}\right)=0.18\left(\frac{B_{eff}}{B}\right)^3-\left(\frac{B_{eff}}{B}\right)^2+1.91\left(\frac{B_{eff}}{B}\right)-0.13 \quad (9)$$

$$1<\frac{B_{eff}}{B}<3.05\ ,\ K\left(\frac{B_{eff}}{B}\right)=1\ ,\ \frac{B_{eff}}{B}=1$$

$$K\left(\frac{B}{d_{50}}\right)=\left(0.045\left(\frac{B_{eff}}{B}\right)^{0.18}\right)\times\left(13.3+0.016\left(\frac{B}{d_{50}}\right)^{1.55}\right) \quad (10)$$

$$5<\frac{B}{d_{50}}<50\ ,\ K\left(\frac{B}{d_{50}}\right)=1\ ,\ \frac{B}{d_{50}}\geq 50$$

Eq. (8) can be used for $3<B/d_{50}<67$ and $1<B_{eff}/B<3.05$ and $1<y/B<10$. Figure 7 shows the accuracy of Equation (8) in predicting the experimental data. The experimental data presented by previous studies are also included in Figure 7. As shown in Figure 7, a 10% decrease in U/U_c covers all of the present, and Karimaee and Zarrati (2013), experimental data. Therefore, a coefficient equal to 0.9 is multiplied to the right hand side of Eq. (8) to attain the envelope of all tests (no failure condition in all tests). In addition, a 20% decrease in U/U_c or multiplying 0.8 to the right hand side of Eq. (8) covers all of the available experimental data (no failure) presented in Table 2 (Figure 7).

Algorithm for Riprap Design

Design of riprap stone by Eq. (8) needs a trial and error process with the following steps:

1. With assuming U/U_c = 0.35 as initial guess and knowing U, calculate riprap size from Eq. (3).
2. Using the calculated d_{50}, the parameters $K(B_{eff}/B)$ and $K(B/d_{50})$ can be found from Eqs. (9) and (10) respectively; finally, the parameter U/U_c can be calculated again from Eq. (8).
3. A new value for d_{50} can then be calculated from Eqs. (1) to (3) according to the value of D* in Eq. (5).
4. Steps (2) to (4) are repeated in order to get a constant d_{50}.

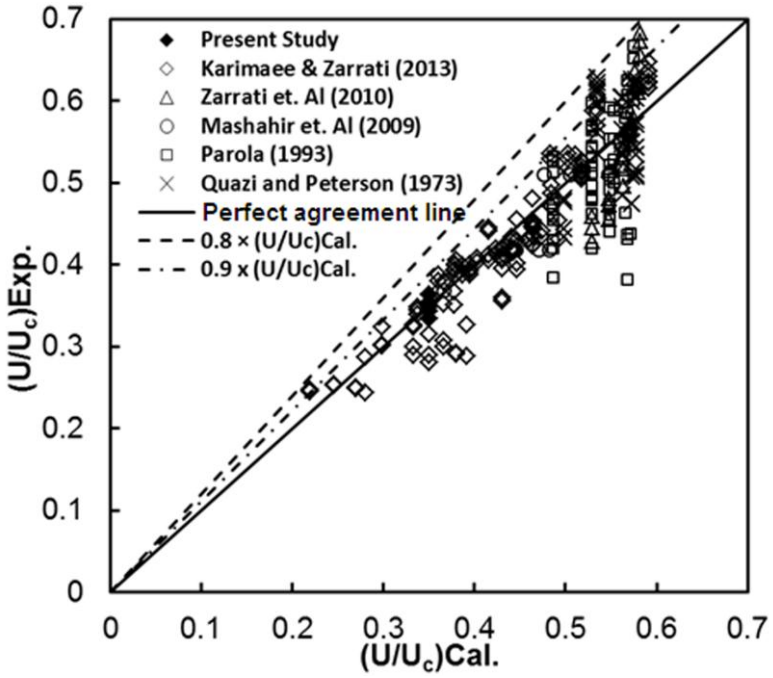

Fig. 7. Comparison of the experimental data with Eq. (8).

ARTIFICIAL NEURAL NETWORK

Empirical equations based on regression analysis are not able to include all complex relationships between the involved parameters in one equation. This is true especially since the critical regions of riprap failure are different under different flow and riprap size conditions (Karimaee and Zarrati, 2013). In recent years, artificial intelligent techniques such as artificial neural network (ANN), genetic algorithm, and neuro fuzzy systems are widely used to address various complex problems in different fields of engineering (Hsu, 2011). As is shown in Figure 8, a typical structure of ANN consists of a number of processing elements or nodes that are usually arranged in an input layer, an output layer and one or more hidden layers. The nodes receive inputs from the initial inputs and produce outputs by the transformation using an adequate nonlinear transfer function *f(x)*. The effectiveness of an ANN model to simulate a highly nonlinear problem is attributed to the nonlinear transfer function (Shin and Park, 2010). A common transfer function is the sigmoid function expressed by $f(x)=1/1-e^{-x}$, which has a characteristics of $df/dx=f(x)[1-f(x)]$.

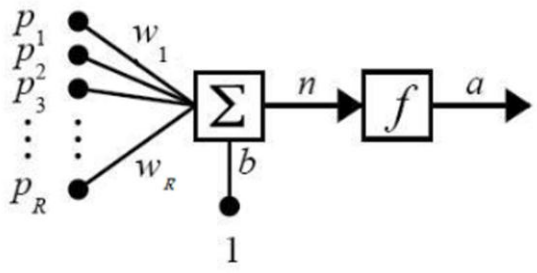

Fig. 8. Structure of an artificial neural network.

Previous studies showed that ANN has provided reasonably good solutions for hydraulic engineering problems, particularly for the cases of a highly nonlinear and complex relationship between the input-output pairs in the corresponding data (Muzzamil and Siddiqui, 2003; Azamathulla et al., 2005). In the literature, there are ample of studies into applying ANN in predicting scour depth around bridge piers (Kambekar and Deo, 2003; Bateni et al., 2007; Shin and Park, 2010). However, riprap sizing around a bridge pier employing ANN has not been considered yet.

In the present study, the multi-layered feed forward-back propagated network (Levenberg–Marquardt) was used in an ANN method for predicting the stable riprap size. Hornik et al. (1989) stated that multilayer feed forward networks (FFN) with as few as one hidden layer are indeed capable of universal approximation in a precise and satisfactory sense. They also concluded that if there is any lack of success in applications, this fact might arise from inadequate learning, insufficient numbers of hidden units, or the lack of a deterministic relationship between input and output. Of all the available data, 70% (more than 190 experimental data, shown in Table 2) were randomly selected for training the networks and the 30% of the remaining data were used for testing and for evaluating the networks (15% for test and 15% for evaluation). In order to make the present ANN model capable in real prototype cases, all data were used in a non-dimensional form. The method was, therefore, composed of training of ANN with B/d_{50}, B_{eff}/B and y/B as inputs and the flow intensity parameter (U/U_c) as the output. From U/U_c the riprap size could then be calculated from Eqs. (1) to (3). In addition, different training methods such as multi-layer perception (MLP) or radial basis function (RBF) were developed for predicting the flow intensity parameter in riprap stone failure conditions. The results showed that the best performance could be assessed by MLP network. According to Muzzammil and Siddiqui (2003) and Azamathullah et al. (2005), MLP networks are more suitable networks for the hydraulic phenomena.

The next step was to select the number of hidden layers and the number of neurons in each hidden layer. The use of one hidden layer is generally recommended, at least in preliminary studies, because by increasing the number of hidden layers the training process slows down without substantially improving the efficiency of the network. According to the number of neurons in the layers, many networks were developed and tested. The structural details of the best networks are given in Table 3. In addition, the configuration of the designed ANN is shown in Figure 9. The ANN predictions were then compared with Eq. (8). For this comparison, the criteria mean-absolute error (MAE), root-mean-square error (RMSE) and coefficient of determination (R^2) were used and the results are given in Table 4. According to this table, ANN model is more accurate than the regression model (Eq. (8)). Figure 10 shows the best agreement between the measured and estimated values for the ANN model. All of the data were confined within ±15% intervals along the trend line, which shows the higher accuracy of the ANN model compared with the regression model shown in Figure 7. Therefore, for design purposes the calculated U/U_c in the ANN model must be multiplied by 0.85 to cover all experimental data.

The weights and biases for the MLP are given in Table 5. It must be noted that, similar to the regression model, a riprap design with presented ANN model is also a trial and error method. The steps are similar to those cited for the regression model. However, in the ANN model, instead of Eq. (8) for calculating U/U_c, the ANN network with weights and biases presented in Table 5 must be used.

Table 3. Algorithm of ANN scheme for riprap design.

Neural Network Learning Algorithm	Network Structure		
	Number of Input Layer Neurons	Number of Middle Layer Neurons	Number of Output Layer Neurons
MLP	3	10	1

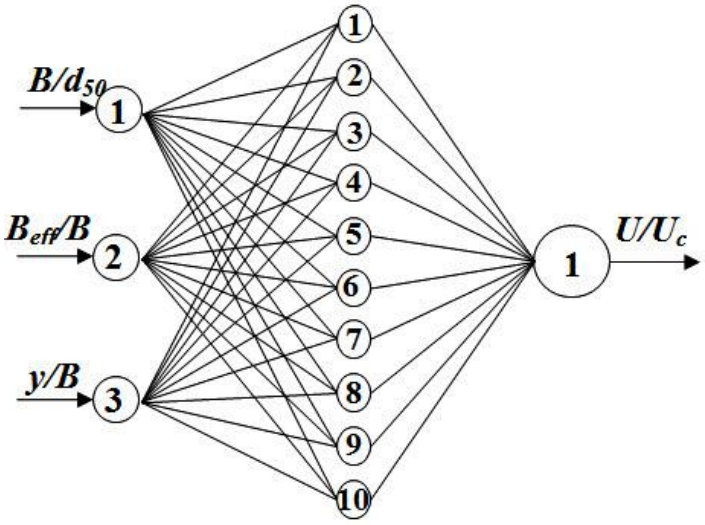

Fig. 9. Network architecture for the ANN model.

Table 4. Performance evaluations of various models for riprap design.

Model	Error Criteria		
	MAE	**RMSE**	**R^2**
ANN	0.030	0.042	0.91
Regression	0.035	0.047	0.85

Note: MAE, RMSE and R^2 stand for mean-absolute-error, root-mean-square error and R-Squared values

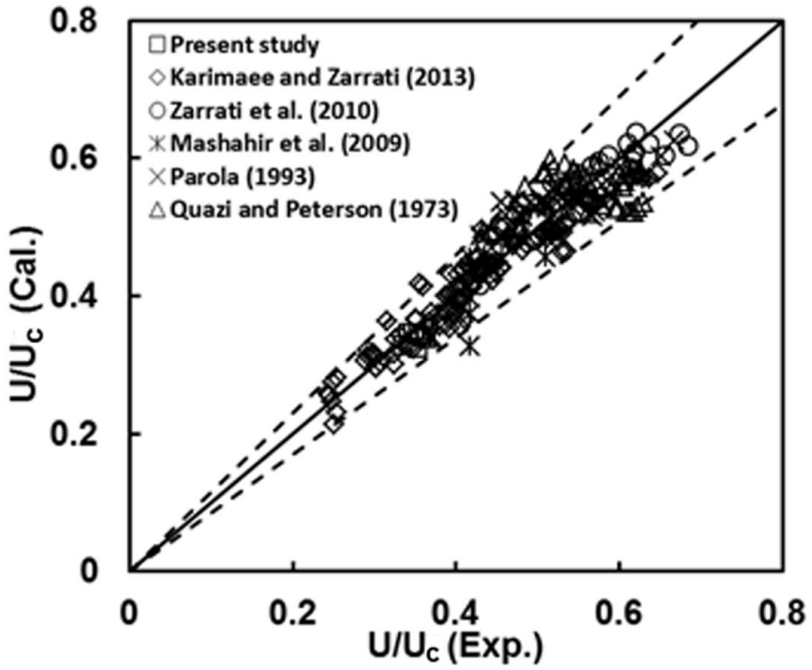

Fig. 10. Comparison of experimental data and ANN predictions.

Table 5. Details of weights and biases for MLP model.

Hidden Layer	Weights (I= input; O= output)				Biases	
	I			O	I	O
	1	2	3			
1	0.34	0.24	-1.23	-0.26	0.38	0.19
2	1.17	-1.54	-1.93	0.28	0.49	
3	0.36	0.53	0.33	0.41	0.04	
4	-0.72	0.97	1.30	0.09	0.12	
5	0.29	1.05	-0.01	1.14	-1.08	
6	0.74	0.86	-1.80	-1.65	-0.93	
7	-1.37	-0.10	-1.36	-0.05	0.27	
8	-0.22	-0.89	0.79	0.69	-0.60	
9	0.75	-0.34	-1.38	1.75	1.09	
10	-0.64	-0.92	-1.19	0.88	-0.41	

SENSITIVITY ANALYSIS

Sensitivity analysis is commonly carried out to determine the relative significance of each independent parameter (input neurons) on the dependent parameter (output neurons). For this purpose ANN models were developed each time without one of the independent parameters. The results of sensitivity analysis are shown in Table 6. This table indicates that (B_{eff}/B) and (y/B) are the most and least effective parameters

on the critical flow intensity (U/U_c). The same conclusion was made by analysing experimental data for regression analysis.

Table 6. Sensitivity analysis results.

Model	MAE	RMSE	R^2
ANN	0.030	0.042	0.91
ANN without y/B	0.036	0.047	0.89
ANN without B/d_{50}	0.051	0.065	0.76
ANN without B_{eff}/B	0.066	0.084	0.54

Comparison of the Present Model with Previous Empirical Equations

Comparison of the developed empirical equation and the ANN method considering the reduction coefficients introduced for U/U_c (0.8 for Eq. (8) and 0.85 for ANN), with other empirical equations (Table 1) in predicting stable riprap size using all experimental data (Table 2) is shown in a box-and-whisker diagram presented in Figure 11. This diagram includes five different numbers i.e., the smallest observation, lower (Q1), median (Q2), and upper quartile (Q3), and largest observation. Spacing between different parts of the boxes helps to indicate the degree of dispersion (spread) and skew (asymmetry) of the prediction errors. In addition, the interquartile range (IQR) that is IQR = Q3-Q1 is an important part that shows the dispersion of the prediction errors. The experimental data include the circular pier as well as the aligned round-nose-and-tail rectangular pier. As is shown in this figure, the best predictions of experimental data are for the ANN model, as its estimates are well-balanced and limited between 1 and 2.3 times the experimental value with an average close to 1.55. It can be noted that with using ANN the predicted riprap size has been always more and close to the experimental stable riprap size. In addition, all of the results by Eq. (8) are also larger than 1 and limited between 1 and 2.9 times the experimental value with an average close to 1.76. The results for the Karimaee and Zarrati (2013) equation have the lowest IQR or dispersion with a median value of 1.35.

However, the Breuseres et al. (1977) equation in general over-predicts the stable riprap size with a median value of 7.41. Predicted riprap sizes by Quazi and Peterson (1973), Parola (1993), Croad (1997), and Froehlich (2013) are below the experimental sizes (calculated/measured d_{50}<1) in some ranges of flow conditions.

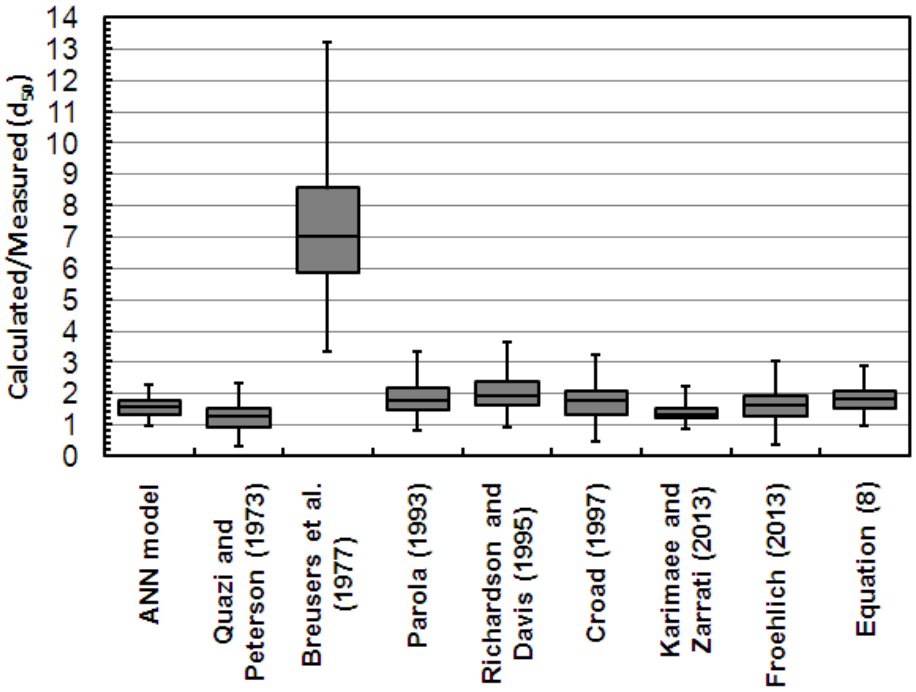

Fig. 11. Box-and-whisker diagram comparing the ratios of calculated and measured riprap size.

CONCLUSIONS

In the present study, the stability of riprap stones around circular as well as aligned and skewed round-nose-and-tail rectangular bridge piers was studied based on a large amount of experimental data. In addition to previous experiments, new experiments were also conducted for larger pier width to riprap size ratio, which was not available in the literature. Based on experimental data, effects of important parameters including relative flow depth, relative stone size and effective pier width on the value of flow intensity parameter (U/U_c) in riprap instability conditions were studied. It was concluded that parameters B_{eff}/B and y/B have the highest and lowest effects on riprap stability condition, respectively. Experiments showed that, for the aligned pier, by decreasing the parameter B/d_{50} from 62.5 to 7.14, the value of U/U_c increased about 82%. However, in the case of B/d_{50}=35.71, by increasing the parameter B_{eff}/B from 1 to 3.4, the parameter U/U_c decreased by about 45%. The experimental data were then analysed and an equation was developed based on effective parameters by multiple regression analysis to estimate the stable riprap stone size around bridge piers. The ratio of predicted to experiment riprap size value for all experimental data is larger than 1 with an average value of 1.75, which is less than many other empirical equations. In addition, in order to get a more accurate method for riprap design, an artificial neural network (ANN) based on utilizing non-dimensional parameters was deployed. Sensitivity analysis of effective parameters in developing the ANN model confirms the highest effect of pier effective width on riprap stability. Finally, the comparisons between the present methods and other empirical equations showed that the ANN model provides the best prediction for riprap size.

LIST OF NOTATION

B: Pier width
y: Flow depth
U: Flow velocity
U_c: Critical velocity for riprap stone movement
B: Pier width
L: Pier length
θ: Pier skew angle or flow angle of attack
B_{eff}: Pier effective width
d_{50}: Riprap stone size
g': Reduced gravitational acceleration
D_*: Dimensionless sediment size
σ: Sediment non-uniformity
ν: Water kinematic viscosity
R_h: Hydraulic radius of the channel
ρ: Fluid density
ρ_s: Sediment density
$K\left(\frac{B_{eff}}{B}\right)$: Modification factor for relative pier width
$K\left(\frac{B}{d_{50}}\right)$: Modification factor for relative riprap stone size

REFERENCES

Azmathullah, H.M., Deo, M.C. and Deolalikar, P.B. (2005). "Neural Networks for estimation of scour downstream of a ski-jump bucket", *Journal of Hydraulic Engineering*, 131(10), 898-908.

Breusers, H.N.C., Nicollet, G. and Shen, H.W. (1977). "Local scour around cylindrical piers", *Journal of Hydraulic Research*, 15(3), 211–252.

Bateni, S.M., Jeng, D.S. and Melville, B.W. (2007). "Bayesian neural networks for prediction of equilibrium and time-dependent scour depth around bridge piers", *Advance in Engineering Software*, 38(2), 102-111.

Chiew, Y.M. and Melville, B. (1987). "Local scour around bridge piers", *Journal of Hydraulic Research*, 25(1), 15-26.

Chiew, Y.M. (1995). "Mechanics of riprap failure at bridge piers", *Journal of Hydraulic Engineering*, 121(2), 635-643.

Croad, R.N. (1997). *Protection from scour of bridge piers using riprap*, Transit New Zealand Research Report No. PR3-0071, Works

Consultancy Services Ltd., Central Laboratories Lower Hutt, New Zealand.

Froehlich, D.C. (2013). "Protecting bridge piers with loose rock riprap", *Journal of Applied Water Engineering and Research*, 1(1), 39-57.

Gaudio, R., Tafarojnoruz, A. and Calomino, F. (2012). "Combined flow-altering countermeasures against bridge pier scour", *Journal of Hydraulic Research*, 50(1), 35-43.

Hager, W. H. and Oliveto, G. (2002). "Shields entrainment criterion in bridge hydraulics", *Journal of Hydraulic Engineering*, 128(5), 538–542.

Hornik, K., Stinchcombe, M. and White, H. (1989). "Multilayer feed forward networks are universal approximates", *Neural Networks*, 2(5), 359–366.

Hosseini, S.H., Hosseinzadeh Dalir, A., Farsadizadeh, D., Arvanaghi, H. and Ghorbani, M.A. (2011). "Application of submerged vanes to control scouring around rectangular bridge piers", *Civil Engineering Infrastructures Journal*, 45(3), 301-310.

Hsu, K.L. (2011). "Hydrologic forecasting using artificial neural networks: a Bayesian sequential Monte Carlo approach", *Journal of Hydroinformatics*, 13(1), 25-35.

Kambekar, A.R. and Deo, M.C. (2003). "Estimation of group pile scour using neural networks", *Journal of Applied Ocean Research*, 25(4), 225-334.

Karimaee Tabarestani M. and Zarrati A.R. (2013). "Design of stable riprap around aligned and skewed rectangular bridge piers", *Journal of Hydraulic Engineering*, 139(8), 911-916.

Karimaee Tabarestani M. and Zarrati A.R. (2011). "Effect of collar on time development and extent of scour hole around cylindrical bridge piers", *International Journal of Engineering, Transactions C*, 25(1), 11-16.

Kirkgoz S. and Ardichoglu M. (1997). "Velocity profiles of developing and developed open channel flow", *Journal of Hydraulic Engineering*, 123(12), 1099-1105.

Lagasse, P.F., Clopper, P.E., Zevenbergen, L.W. and Girard, L.G. (2007). "Countermeasures to protect bridge piers from scour", *NCHRP Report 593*, TRB, NAS, Washington D.C., 272p. www.trb.org.

Lauchlan, C.S. and Melville, B.W. (2001). "Riprap protection at bridge piers", *Journal of Hydraulic Engineering*, 127(5), 412-418.

Lee, S.O. and Sturm, T.W. (2009). "Effect of sediment size scaling on physical modeling of bridge pier scour", *Journal of Hydraulic Engineering*, 135(10), 793-802.

Mashahir, M.B., Zarrati, A.R. and Mokallaf, E. (2009). "Application of riprap and collar to prevent scouring around piers rectangular bridge", *Journal of Hydraulic Engineering*, 136(3), 183-187.

Muzzammil, M. and Siddiqui, R. (2003). "An artificial neural network model for scour prediction: Advances in Civil Engineering", *Prospective of Developing Countries*. Vol. II., Parmar and Kumar (ed.), 430–441, Alied Publishers Pvt. Limited.

Parola, A.C. (1993). "Scour protection at bridge piers", *Journal of Hydraulic Engineering* 118(2), 1260-1269.

Quazi, M.E., and Peterson, A.W. (1973). "A method for bridge pier riprap design", *Proceedings of 1st Canadian Hydraulic Conference*, Edmonton, AB, pp. 96–106.

Raudkivi, A.J. (1998). *Loose boundary hydraulics*, Balkema, Rotterdam, The Netherlands.

Richardson, E.V. and Davis, S.R. (1995). "Evaluating scour at bridges", *Hydraulic Engineering Circular (HEC)*, No. 18, FHWA-IP-90-017, Fairbank Turner Hwy. Res. Ctr., McLean, Va.

Sheppard, D.M., Odeh, M. and Glasser, T. (2004). "Large scale clear-water local pier scour experiments", *Journal of Hydraulic Engineering*, 130(10), 957-963.

Shirole, A.M. and Holt, R.C. (1991). *Planning for a comprehensive bridge safety assurance program*, Transportation Research Record 1290, Transportation Research Board, Washington, D.C., 137–142.

Shin, J.H. and Park, H.I. (2010). "Neural network formula for local scour at piers using field data", *Marine Georesources and Geotechnology*, 28(1), 37-48.

Soltani-Gerdefaramarzi, S., Afzalimehr, H., Chiew, Y.M. and Lai, J.S. (2013). "Jets to control scour around bridge piers", *Canadian Journal of Civil Engineering*, 40(3), 204-212.

Tafarojnoruz, A., Gaudio, R. and Calomino, F. (2012). "Bridge pier scour mitigation under steady and unsteady flow conditions", *Acta Geophysica*, 60(4), 1076-1097.

Zarrati, A.R., Gholami, H. and Mashahir, M.B. (2004). "Application of collar to control scouring around rectangular bridge Piers", *Journal of Hydraulic Research*, 42(1), 97-103.

Zarrati, A.R., Chamani, M.R., Shafaei, A. and Latifi, M. (2010). "Scour countermeasures for cylindrical bridge piers using riprap and combination of collar and riprap", *International Journal of Sediment Research*, 25(3), 313–321.